Heliyon 10 (2024) e27407

Contents lists available at ScienceDirect

Heliyon

journal homepage: www.cell.com/heliyon

Research article

# Research on the parameter design and calibration and control of EV in-vehicle active sound generation system

Shuai Zhang [a], Yipeng Li [a], Hang Jiang [a], Feng Xiong [b], Liyou Xu [a,*], Yuntao Cao [c]

[a] College of Vehicle and Traffic Engineering, Henan University of Science and Technology, Luoyang, 471003, China
[b] College of Vehicle Engineering, Chongqing University of Technology, Chongqing, 400054, China
[c] State Key Laboratory of Comprehensive Technology on Automobile Vibration and Noise & Safety Control, Changchun, 130022, China

A R T I C L E I N F O

*Keywords:*
EV
Uniform speed conditions
Sound quality
Calibration method
Active control system

A B S T R A C T

In order to improve the interior sound quality of electric vehicles (EVs) under acceleration and uniform speed conditions, to balance the comfort and dynamics of the interior sound, and to improve the accuracy and performance of the active sound generation system (ASGS), this article carries out the research related to the parameter design, sound calibration, evaluation methodology, and control system of the EV ASGS. Propose an in-vehicle sound design method focusing on three dimensions, including engine order composition, spectral energy distribution, and sound amplitude enhancement in the typical speed range, and determine the in-vehicle sound design scheme and the total sound value target. Focus on the sound parameter design, calibration and evaluation methods of EV ASGS considering the frequency response characteristics of the loudspeaker, sound amplitude control accuracy, sound quality, and psychoacoustic parameters, clarify the active sound parameter settings of EVs, complete the analysis of sound extraction methods, complete the engine order sound fitting, and design the ASGS of the EV interior by combining the subjective and objective evaluations. Develop the control software and hardware of the ASGS, complete the construction and accuracy verification of the ASGS based on the in-vehicle sound system, and realize the sound calibration of the ASGS under the static conditions of the real vehicle and the verification of the target achievement. The real-vehicle test shows that the ASGS reduces the sharpness of 1.0 acum and 0.52 acum under acceleration and constant speed conditions, respectively, and improves the comfort and dynamics of in-vehicle sound. The objective and subjective evaluation results show that the parameter design, selection and accuracy of the sound calibration and evaluation methods of the ASGS in the EV determines the accuracy and effect of the ASGS.

## 1. Introduction

The vehicle has many characteristics such as lightweight and NVH performance [1,2]. Further customer requirements for vehicle quality promote the evolution of NVH control measures from reducing fundamental vibration and noise amplitude to evaluating sound quality for diminishing the annoying sound and finally to advancing sound design.

Active sound technology is the core of the technology of future EV sound design, which is able to enhance the sound quality and provide a diversified listening experience in the vehicle to adapt to customers' preferences. Therefore, carrying out the research on

* Corresponding author.
*E-mail addresses:* lyp1154437581@163.com (Y. Li), xiongfeng@cqut.edu.cn (F. Xiong), xlyou@haust.edu.cn (L. Xu), caoyt18@126.com (Y. Cao).

https://doi.org/10.1016/j.heliyon.2024.e27407
Received 26 May 2023; Received in revised form 27 November 2023; Accepted 28 February 2024
Available online 14 March 2024

active sound technology takes on enormous significance.

The sound quality of the car determines the mood of the occupants. Ma, CG. et al. [3] proposed a sensitive critical band diagnosis method of permanent magnet synchronous motor (PMSM) in electric cars. Mosquera-Sanchez, JA. et al. [4] established a framework for improving the quality of noise perception in hybrid systems in passenger cabins. Loudness, roughness, and sharpness were used as key performance indicators for evaluating optimization effectiveness. As reported by experimental results of the proposed framework, the success rate for improving the sound quality at several aspects in the vehicle model is more than 90%. Different driving conditions can produce different subjective perceptions. Doleschal, F. et al. [5] explored the extent of their influence on the perception of synthetic sound through a variety of driving conditions. Swart, DJ. et al. [6] indicated that the sound quality in the interior of EVs had an impact on the individual driving pleasure and vehicle's market acceptance, and proposed a new consumer satisfaction index based on interior sound features they have long studied. Wagner-Hartl, V. et al. [7] conducted a study in which multiple testers evaluated the different sounds produced by electric vehicles as they accelerated and decelerated from higher speeds on test roads and public roads, in order to more clearly judge the sound changes of electric vehicles. Min, D. et al. [8] synthesized artificial engine sounds by combining mechanical sounds and combustion sounds. To evaluate the efficacy of created sounds important parameters were measured, and auditory experiments, moreover, were performed to determine the recognizability and perceptual impression of sounds in the context of vehicle proximity. HEE et al. [9] introduced the implementation of sound absorbing materials in EVs that can effectively reduce noise levels and create a more pleasant and comfortable driving environment for driver and passenger. This was supported by a noise index for subjective evaluation of such materials, the index they developed based on the masking theory.

The improvement of sound quality attracts increasing attention for addressing noise pollution and enhancing safety. Through the study of sound quality, an index to evaluate sound motion characteristics was studied by Park, JH. et al. [10]. The new indicators are verified and analyzed by the new samples. Through a variety of optimization methods, a sound quality prediction method based on PSO -BPNN was studied by Zhang, EL. et al. [11]. And the test shows that this method can improve the precision of sound quality and the convergence speed is faster. Jeong, JE. et al. [12] suggested a new evaluation index based on the Mahala-nobis distance using four parameters Zwicker employed to estimate the subjective perception of sound quality. Through a correlation analysis with jury tests, it was found that the logarithmic Mahala-nobis distance can serve not only as a novel index but also as a reliable criterion for evaluating. A new method was investigated by Wang, ZH. et al. [13], which relies on a method of human ear basilar membrane displacement, and two BP neural network models were developed in order to test the sound quality in vehicles. The new metric called SMVBMDR can be used as a valid parameter to better objectively assess quality. Zhuang, T. et al. [14] gathered vehicles' sound signals through designing their different driving speed on the highway, the replay of collected signals with the help of the playback software HEAD Audio Recorder. The evaluation model was established by SPSS analysis software to compare and correlate objective measurements of psychoacoustic parameters with the results of subjective evaluations of sound quality that were tested by paired comparison method. Lu, Y. et al. [15] based on CEEMD, introduced a new approach to sound test. The evaluation at the power coupling mechanism of HEV was through HT and RVM. Lee, YJ. et al. [16] presented a study that shed light on the connection the way vehicles' sounds are perceived by humans and tee physical properties that underline those perceptions. For further comprehending the relationship between subjective evaluation and objective measures of sound characteristics, statistical analysis was performed, using principles of psychoacoustics and additionally, by the technique of electroencephalogram (EEG), the correlation between an individual's subjective perceptions and brain activity was measured. A new evaluation system based on biological signals was developed for vehicles. Lee, SK. et al. [17] formulated a model to predict how acoustic properties of vehicle's interior are affected by changes in the physical properties of sound absorbing materials in the side wall of a virtual automobile engine compartment, and the method was confirmed to work as expected in an experiment tested in a real-world condition.

Thanks to the fact that the technology in ASGS is constantly upgrading, the sound of vehicle's interior becomes more enjoyable. Ghanati, G. et al. [18] designed an sound control system, and proposed a robust feedback control strategy using multiple inputs and outputs to reduce SPL experienced by all occupants. Anthony, M. et al. [19] introduced an ANC system, performing real-time experiments. The ANE was also conducted experiments to achieve the sound adjustment of the engine. An active sound quality control method based on local sub-path estimation and filtering error structure was investigated by Chen, W. et al. [20], and the modified scheme achieved and optimized the sound quality inside the vehicle during acceleration. Wang, Y. et al. [21] developed a framework using an online quadratic path modeling approach to design active sound systems. Building upon the foundation of existing algorithms, an ASS-LMS algorithm for quadratic path modeling with interference signals is drafted, whose efficacy was proved by the simulation results. An improved auxiliary noise power scheduling strategy is, moreover, outlined. An active control method was investigated by Liu, F. et al. [22], which is able to accurately control SPL of the residual noise when the interference noise amplitude is changed by shaping the spectrum of the residual noise according to the filter to achieve the design scheme. Lee, SK. et al. [23] outlined a new method of active noise cancellation (ANC) to deaden the engine whine in vehicles and it could work steadily at high-speed variations. They then demonstrated that the ANC system with the new method was capable of reducing the intensity of engine noise, by simulating and comparing the new and the conventional method through three synthetic signals. Wang, YS. et al. [24] established a piezoelectric feedback system for ANC a useful tool to offer faster and more accurate noise cancellation, and improved FXLMS algorithm utilizing DWT.

Yu, WT. et al. [25] optimized the EV running at 40 km/h through experiments and simulations, and added a dynamic vibration absorber to resonate at a modal frequency of the acoustic cavity, but with an opposite phase so as to cancel out the vibration that led to unwanted noise and even the damage of the structure if they are strong enough. In the evaluation of the absorber, the overall noise level of a vehicle, at a frequency of 42Hz, was reduced by 8dBA, and this reduction in noise level corresponded to a decrease in the ear pressure level, thereby the NVH performance being improved. Liu, ZE. et al. [26] studied evaluation way of strong quality and the strategy of vehicle noise target, applied the subjective evaluation method of continuous evaluation based on predefined categories to subjective evaluation, and proposed the development process for strong sound target. An AST method was investigated by Feng, T. et al. [27], which piggybacks on the frequency domain inverse model LMS algorithm to reshape the response of the vehicle powertrain according to the sound quality requirements designed. The effectiveness of the method was verified by performing noise signal simulation tests with the vehicle powertrain. Wu, SL. et al. [28] designed a new method to control the external noise EVs produced at acceleration through measuring sound intensity. As a result of the new method, mistakes made in the noise control occurred less frequently than before, and the time taken in this method was shorter, both of which greatly contributed to the control effect. LEE, JK. et al. [29] under two test conditions as vehicle was at full throttle or at the constant speed, suggested the most critical factors of the test and an index for the evaluation of driving environment, through which a corresponding equation was obtained by multi-factor regression method. Zeng, FL. et al. [30] used the ZSSTV method to establish a GA-BP sound prediction model, based on objective parameters and a sound quality parameter SQP-WRW. Their test results demonstrated that the model enjoyed higher accuracy in predicting the quality. Zhang, XJ. et al. [31] tested the sound quality in a car under various conditions by keeping the car at engine idle and using an SVM model. The results can show that the jitter level, loudness, roughness, and sound pressure level are the four main acoustic evaluation indicators. Siano, D. et al. [32] conducted a study on a vehicle's operating conditions and certain areas where passengers were susceptible to the boom phenomenon, by studying the acceleration conditions of a vehicle with a chassis dynamometer The study optimized vehicle sound quality for its contributions to the selection of the most appropriate strategy to control noise and vibration. Moon, S. et al. [33] aimed at deriving the semantic space of quality of sound produced when the engine accelerated for end users and determining the relationship with characteristics. Their research provided a valuable guidance for the development of engine acceleration sounds, which fulfilled the customer's individual preference and stimulated their purchasing desire.

In summary, the sound quality should meet the diversified needs of customers, while active sound technology is the core key technology to realize the sound design of future EVs. The current research mainly focuses on the sound quality of EVs under acceleration or uniform speed conditions, evaluation methods, active sound control systems, etc., and important results have been obtained. And the precision and effect of the ASGS of sound quality in the car depends on the parameter design, sound calibration and evaluation method selection and precision of the ASGS of the car. Therefore, this paper focuses on the research of the sound parameter design, calibration and evaluation methods of the EV ASGS considering the frequency response characteristics of the loudspeaker, the precision of sound amplitude control, and the psychoacoustic parameters of sound quality, and the development of the EV in-vehicle ASGS by combining the subjective and objective evaluations, so as to improve the research of the parameter design, sound calibration, evaluation methods and control technology in the development of the EV ASGS. On this basis, a high-performance EV active sound control system is developed by combining a proposed in-vehicle sound design method.

## 2. Sound design for ASGS

### 2.1. Sound design goals

#### 2.1.1. EVs interior sound concept design goal

The object of analysis is an PEV, and the target demographic for sales consists of youthful consumers. The investigation shows that a pleasant driving environment is the first choice for consumers on acquiring an EV. Women prefer comfort, while men prefer motivation. A compressive and detailed study into engine sound is thus still one of the important research fields for improving quality of EV interior sound to create an outstanding driving experience.

The concept design goal of an PEV is formulated as the in-vehicle sound of the SUV should strike a balance between comfort and power.

#### 2.1.2. EVs interior sound concept design technology route

FVs' interior sound quality is closely related to the engine sound. Different design for engine order sound elicits comfort sound quality that represents a smooth and quiet sound allowing drivers a feeling of relaxation, and power sound quality that represents a sound with sense of strength and energy bringing a feeling of thrill. For the classical engine order sound can accomplish the above conceptual design objectives, the technical route is as follows:

(1) Requirements on two distinct aspects of sound control, comfort and power sense, under different driving conditions are studied. In accordance with the analysis of dynamic driving characteristics of EVs, the relationship between acoustic ambiance and vehicle driving parameters such as speed and accelerator pedal opening is investigated.
(2) The sound design method of acceleration engines based on subjective perception is studied, and the influence of different engine order components on subjective sound perception is analyzed. NVH subjective evaluation engineers were organized to evaluate and score, determine the design scheme that meets the conceptual goals, and set the objective goals.
(3) The method of active sound control in EVs is studied. Objective parameters are used to characterize the voice demand of comfort and power sense, and the dynamic sound control of the acoustic atmosphere is realized through the ASGS in the vehicle.
(4) The calibration method of active sound in EVs is studied to verify whether the synthesized sound meets the requirements of synthesis accuracy. The sound calibration and evaluation method of the ASGS in EVs is established, and the objective results of the ASGS are verified by the actual vehicle test.
(5) NVH subjective evaluation engineers are organized to conduct real vehicle evaluations to confirm the achievement of the concept goal of sound. Fig. 1 is the technical route.

### 2.2. Research on comfort and power sound control needs

The simulation of engine sound run by ASGS in the vehicle helps realize, the following sound control requirements under different driving conditions:

When the acceleration of the vehicle is in progress, the simulate the change in the engine order sound to should accurately reflect the acoustic ambiance of power. Additionally, the amplitude should be reasonably controlled when it dynamically responds to the vehicle's acceleration. It is necessary to find a suitable balance that can satisfy both sound quality requirements.

When traveling at a uniform velocity, the acoustic ambiance of comfort is reflected by preserving the original EV amplitude as closely as possible. At the same time, the appropriate engine order sound is retained to reduce the proportion of the original motor sound energy in the interior of the vehicle, so as to improve the sharpness and irritability.

### 2.3. In-vehicle sound design

#### 2.3.1. The vehicle sound design guidelines

The sound of the engine is the main source for the overall sound inside the FV under the acceleration condition, which is shown as follows:

(1) Engine sound is greatly influenced by its components and their organization. As components are arranged in the correct order, the resulting sound becomes pleasing to the ear.
(2) In the range of frequency domain, the energy distribution of engine order components also has an important influence on the subjective sound perception. When the engine order energy is concentrated in the middle and high band, the sound quality tends to motion sense. When concentrated at low range, it is power sense.
(3) In the speed range, the engine order sound amplitude increases with the increase of engine speed. When accelerating in the local speed interval, the engine feeds a louder sound back, so as to enhance the quality of the vehicle's power sense sound.

Features of EV in-vehicle sound design in the study are that the subjective assessment process that relies on personal perception is taken as the fundamental principle, and the conducted sound design of the EV in-vehicle ASGS takes three objective dimensions into consideration, respectively, engine order composition, energy distribution in the frequency domain, and sound amplitude enhancement.

#### 2.3.2. Sound evaluation

A team for subjective assessment is established, whose members consist of seasoned NVH engineers, and the assessment indicators for sound quality are the perceived power and comfort of the sound. The categorization of subjective evaluation score into grades is listed in Table 1.

The test is performed by collecting sound and playing it back. A HEAD Acoustics foreman is used to collect in-vehicle sounds, arranged in front-row, example: Fig. 2. Sound is replayed through the Sennheiser HD650 headset, as depicted in Fig. 3.

Fourteen selected sample vehicles that are tested on a horizontal and smooth road. The EV is engaged into D gear, with the accelerator pedal fully pressed, accelerating from the minimum speed up to 120 km/h while simultaneously collecting the vehicle's sound and the motor speed signal. The FV into 3 gear, accelerating from the corresponding minimum engine speed up to 6000r/min at full load, while recording the sound-speed signal simultaneously.

The sound data of 14 samples are uploaded into the subjective evaluation system, key information such as vehicle brand being

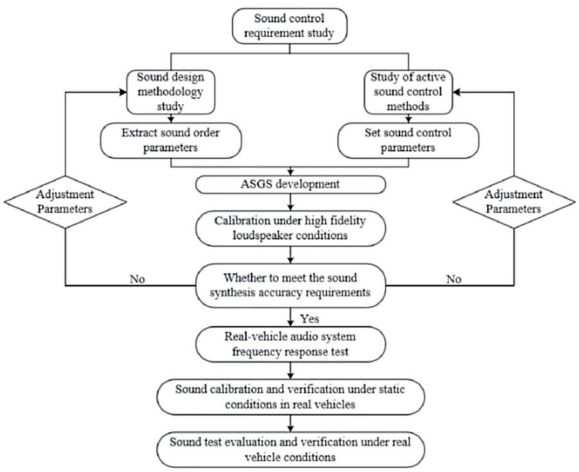


**Fig. 1.** Conceptual design target technical route.

**Table 1**
Score levels.

| Score | Perception | Satisfaction |
|---|---|---|
| 1 | Unacceptable | No quality |
| 2 | | |
| 3 | Very poor | |
| 4 | | |
| 5 | Improvement needed | A little |
| 6 | Acceptable | Basically OK |
| 7 | All right | |
| 8 | Pretty good | Obvious quality |
| 9 | Very good | Very strong quality |
| 10 | Great | |

hidden by random number. Sound samples, therefore, are the only and one marking criterion for evaluators. The results with large deviation are deleted and the average residual score is obtained. The final results are demonstrated in Table 2.

According to Table 3, one of the most prominent aspects of the vehicle 5# is its comfort sound quality, that of vehicle 12# is power sound quality. The 6# and 8# vehicles have kept overall balance between these two aspects.

In order to grasp the influence of engine order composition, the FFT spectrum of 14 sound samples in Fig. 4 analyzes the energy of sound signals distributed across different frequencies and an increase in the amplitude of sound signals at specific speeds.

According to Fig. 4, the sound quality inside the sample vehicle under different acceleration conditions has closely connected to the engine order composition and energy distribution. The perceived comfort of sound quality increases noticeably when the amplitude of engine order component is below 400Hz, which is obvious in the main order (order 3 or order 4) of the engine, clearly, the No. 5 vehicle being the representative. The power level of sound quality is significantly higher when the amplitude of the engine order components exceeds 400Hz. At the same time, the sound amplitude of the main order components of the engine is moderate, obviously, the No. 12 vehicle being the representative.

#### 2.3.3. *Area of sound amplitude enhancement*

The dynamic analysis of driving behavior analysis is carried out. The highly probable consequence of driving with acceleration for the speed interval will be that the in-vehicle sound is characterized with power. For the speed interval with high probability of uniform driving at a constant speed, the sound is featured with comfort. The most likely speed interval in each working condition: Acceleration condition is 40–75 >0–6>15-20(km/h), Uniform velocity condition is 40–80 >0–6(km/h).

### 2.4. *Design scheme*

The Determination of the sound design requirements is as follows:

(1) In the aspect of engine order composition, the fourth order structure is mainly established; and the integer order and half order of other engines are supplemented; The engine order composition should cover the range of 20–1200Hz.
(2) Concerning frequency domain energy distribution, the sound amplitude of engine order component exhibits a higher magnitude below 400Hz, compared to its magnitude at or above 400Hz.
(3) About the enhancement of sound amplitude in typical speed domain, the amplitude of engine order component is enhanced appropriately within the virtual engine speed of 2500-4000r/min.

The change in the amplitude of engine order components should conform to the characteristics of the engine. Engine order

**Fig. 2.** Measuring point of the in-vehicle sound of the HEAD Acoustics foreman.

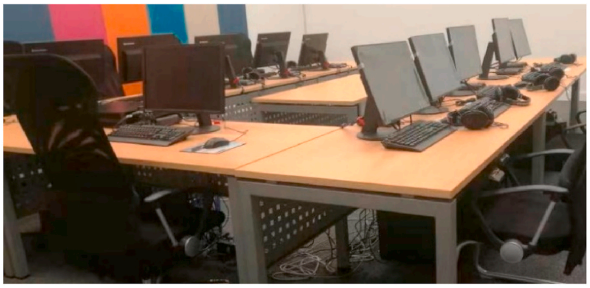

**Fig. 3.** Test and assessment system.

**Table 2**
The evaluation results of the sound in-vehicle during accelerated driving.

| Number | Comfort | Dynamic |
|---|---|---|
| 1 | 7.5 | 8.0 |
| 2 | 8.2 | 7.0 |
| 3 | 6.0 | 6.2 |
| 4 | 7.0 | 7.0 |
| 5 | 8.5 | 7.0 |
| 6 | 7.4 | 7.7 |
| 7 | 5.8 | 5.8 |
| 8 | 7.5 | 7.5 |
| 9 | 7.2 | 6.8 |
| 10 | 7.0 | 6.9 |
| 11 | 8.0 | 6.8 |
| 12 | 7.0 | 8.5 |
| 13 | 7.0 | 7.2 |
| 14 | 6.3 | 5.8 |

**Table 3**
Sound amplitude gain coefficient.

| Engine speed(r/min) | $\alpha[dB(A)\ /100\%]$ | $\alpha_{AVE}[dB(A)\ /100\%]$ |
|---|---|---|
| 3k | 8.1 | 8.5 |
| 4k | 8.5 | |
| 5k | 8.8 | |
| 6k | 8.8 | |

component sounds are constructed in the acoustic processing software Active Sound Design module, and four sound amplitude gain schemes are developed for the virtual engine speed interval of 2500-4000r/min. Fig. 5 depicts the variations in cumulative sound pressure level across fourth scheme change with respect to the engine speed, and Fig. 6 shows the FFT spectrum accordingly.

Subjective evaluation is conducted, as shown in Fig. 7.

In the light of Fig. 7, the results are symmetric, Scheme 1 and 2 exhibits the comfort sound quality, while Scheme 4 is the power sound quality; Scheme 3 selected for the ASGS in EVs can provide both comfort and power.

## 2.5. Total in-vehicle sound target setting

### 2.5.1. Acceleration conditions

The separation of the engine order sounds from the background sounds in an FV is tested. The graph that total value of sound, two sounds are affected by changes in engine speed under 100% accelerator pedal opening is drawn, see Fig. 8.

According to above graph, appropriate adjustment in sound amplitude in the whole speed range of Scheme 3 is made to obtain a different change curve of sound amplitude at maximum accelerator pedal depression, as shown in Fig. 9.

In Fig. 9, the adjusted total sound value retains the sound amplitude enhancement area of 2500-4000r/min, and is consistent with the total value of engine order sound in the FV in the whole area.

### 2.5.2. Constant speed condition

The sound target of the uniform driving condition is set according to the target of the FV engaged the third gear, and aside from such same conditions in speed and gear, the inside sound of the FV is tested within the engine speed of 1000r/min-6000r/min.

For a class-A pure electric SUV studied, the total value of sound, the engine order sound, the background sound and other

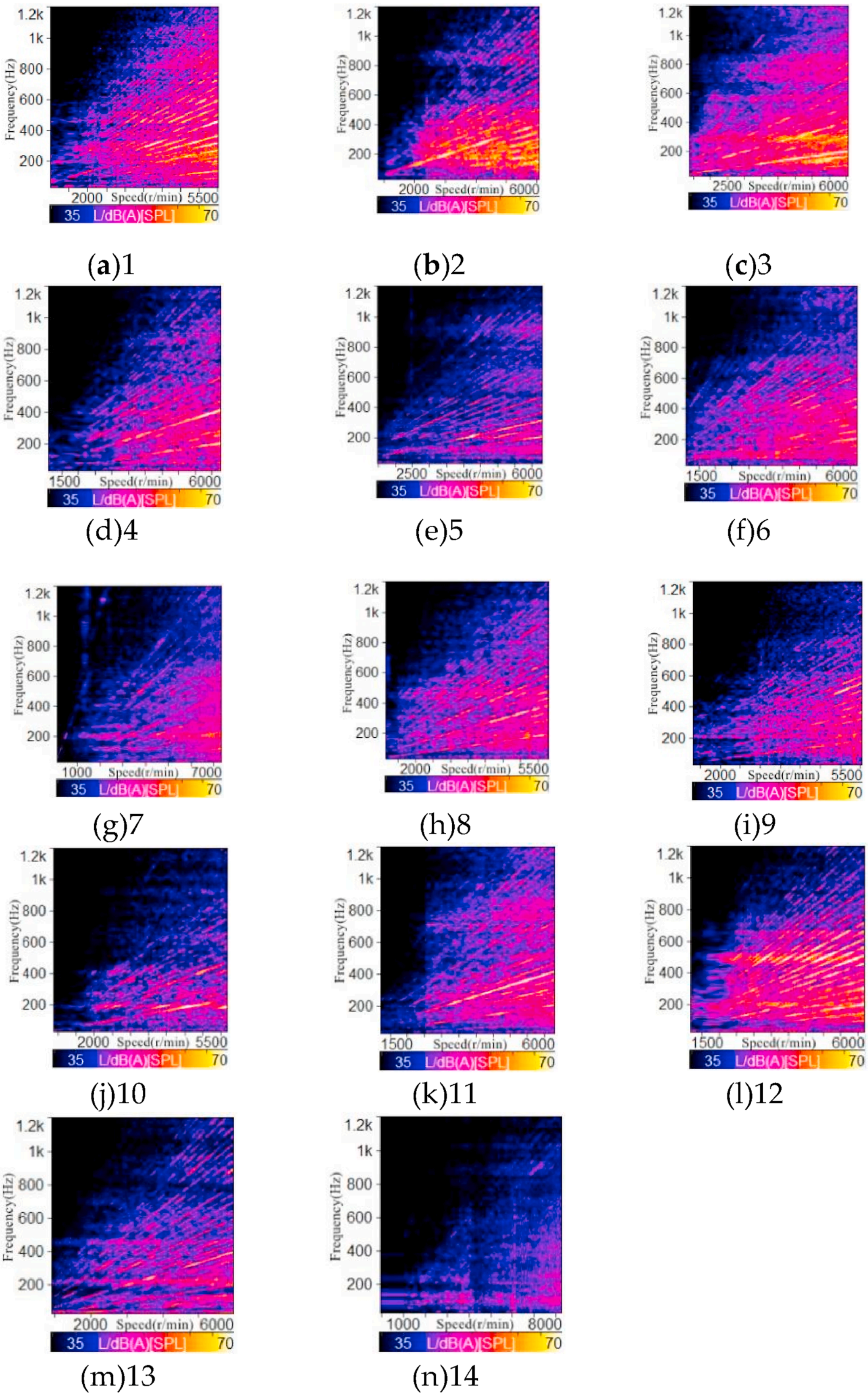


**Fig. 4.** FFT spectrum inside the sample vehicle when it accelerates.

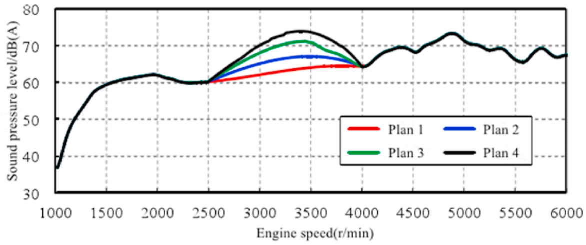


**Fig. 5.** Sound design alternatives.

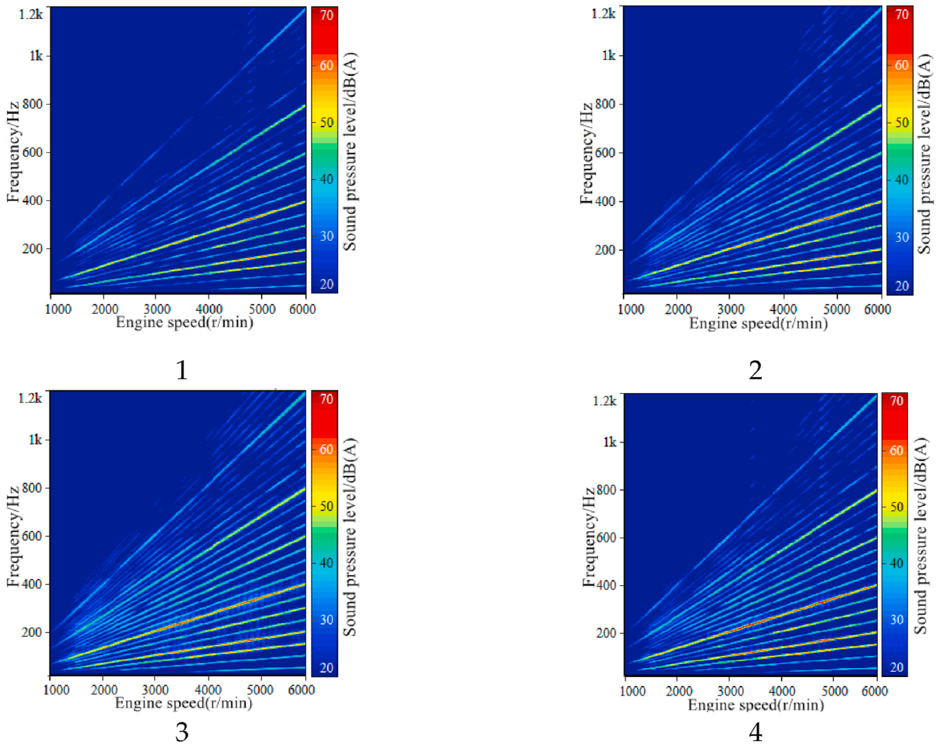


**Fig. 6.** Sound FFT spectrum.

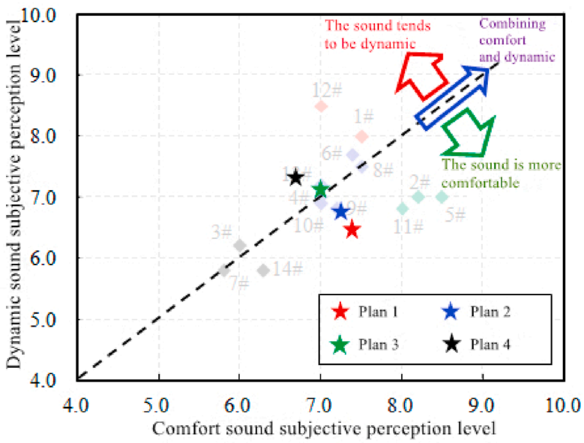


**Fig. 7.** Evaluation results.

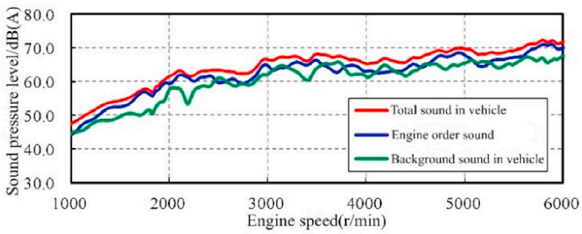


**Fig. 8.** Total amount of sound inside a coupe FV when it accelerates at 100% accelerator pedal opening.

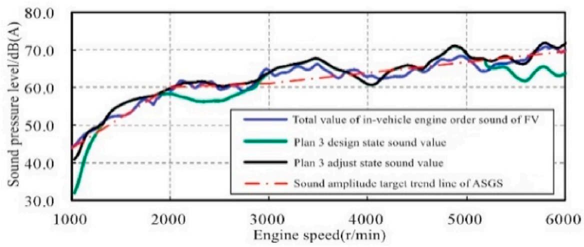


**Fig. 9.** Target curve of total sound value with respect to engine speed in Scheme 3 under 100% accelerator.

information are calculated, example: Fig. 10.

Referring to Fig. 10, the level of the engine order sound and in-vehicle background sound rise linearly in line with engine speed, and the former shows a dramatic growth.

In accordance with the total sound value in Fig. 10, the target of the total sound value of the ASGS and in the vehicle is set based on the original soundtrack in the EV, as shown in Fig. 11.

The blue dashed line serves as the ASGS sound amplitude target line, in Fig. 11, in which the blue dashed line remains situated below the red dashed line of total sound target of EV for the purpose of ensuring noise in the low amplitude and acquire a soothing and pleasant sound.

## 3. Active sound parameters study

### 3.1. Active sound control parameter selection

Speed and pedal opening are selected as voice-activated parameters of the ASGS.

The change of vehicle speed can reflect the change of vehicle running state, and the control system needs to determine the frequency of sound according to the change of vehicle speed Between vehicle speed and sound frequency, the variable of virtual engine speed is set. The virtual engine speed varies in direct proportion to the vehicle speed, as the vehicle speed of 0 km/h corresponds to virtual engine speed 750r/min, and 120 km/h to 6000r/min.

The change of pedal opening can reflect the dynamic characteristics of the vehicle. Different accelerator pedal openings with different frequency of powertrain output result in different amplitude of powertrain sound in the vehicle. Thus, the way to control the sound amplitude is to recognize the opening of accelerator pedal.

### 3.2. Research on sound control method of ASGS

The working steps are as follows:

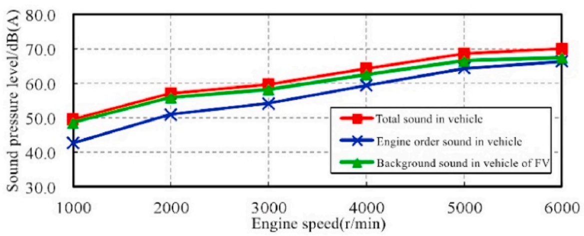


**Fig. 10.** Sound results under uniform driving conditions of FVs.

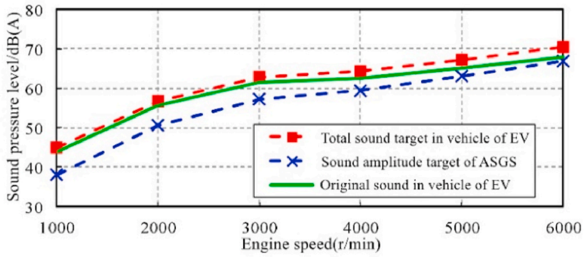


**Fig. 11.** Value of sound and ASGS target.

(1) A suitable FV is used as a reference basis to carry out the research on the test method of in-vehicle engine sound and the dynamic characteristics related to alteration of vehicle's parameters.
(2) The extraction method of order components is studied, and the connection between engine order sound amplitude and accelerator pedal opening is analyzed. The principle for adjusting active sound parameters based on different pedal openings is worked out.
(3) The variation pattern how engine sound amplitude alters with the alteration of vehicle's parameters is analyzed, and the characteristics of EV's parameters and that of FV are compared and analyzed.

### *3.2.1. Correlation analysis between engine sound and vehicle dynamic characteristics in FVs*

The dynamic variation characteristics of the sound inside a coupe FV, respectively comfort and power, are analyzed and studied under different load conditions, with the vehicle for reference purposes.

On the test field's horizontal asphalt road, as the vehicle's transmission is shifted into the second gear, its engine speed quickly increases from 1000r/min to rated speed 6000r/m when accelerator pedal is depressed at 20% opening. Synchronously, in the CAN information, the vehicle speed and engine speed, additionally including engine torque, accelerator pedal opening and other signals are collected. For the investigation of the effects of varying levels of accelerator pedal opening on engine sound, the aforementioned test

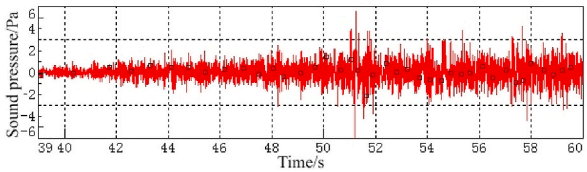


(a) In-vehicle sound test

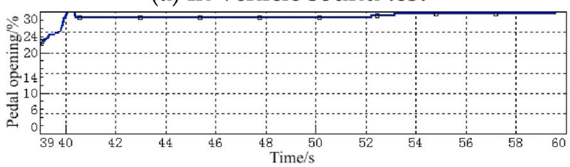


(b) Accelerator pedal opening test

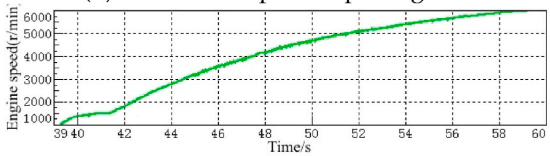


(c) Engine speed test

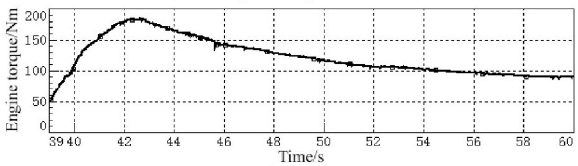


(d) Engine torque test

**Fig. 12.** Time history curves of each signal under 30% pedal opening.

procedures are repeated across a range of accelerator pedal opening from 30% to 100%.

Fig. 12 demonstrates that the sound pressure changes over 21 s at 30% throttle position. The frequency resolution, as shown in Fig. 13.

*3.2.2. Analysis of sound extraction methods*

Direct extraction method: Firstly, the spectrum cloud image is generated through analyzing the data of sound and engine speed measurements. Then the desired engine order is selected using the automatic extraction function. Finally, the unchosen sound components are eliminated and only the chosen engine order components are preserved to facilitate the extraction, as shown in Fig. 14.

Indirect calculation method: Firstly, the spectrum cloud image is obtained according to the first method. Then all prominent engine order components selected in the spectrum are erased, after which wind noise and road noise are left. Finally, the sound data and the erased data are calculated by sound pressure level subtraction method to obtain the order sound data of the engine, example Fig. 15.

Two methods are used to deal with engine order amplitude when the accelerator pedal is depressed to 40% of its maximum range., whose calculation results are compared in Fig. 16.

For the direct extraction method enables engine order components under all acceleration conditions to be extracted, it is applied to calculate the order sound amplitude of engine to enhance the efficiency.

*3.2.3. Analysis of objective evaluation parameters of vehicle acceleration driving power sense*

The power sense experienced during a vehicle's acceleration is a result of the amount of power output from engine. Through the test, the connection of the vehicle acceleration and engine output power under each pedal opening, the changes of characteristics of power sense that results in are analyzed.

Firstly, the discrete vehicle speed data obtained from the test is fitted to the curve, and the multiple power vehicle speed regression equation on the time variable is obtained. Then the differential calculation is carried out to derive the multiple power acceleration calculation equation with respect to the time variable. Finally, the curve describing the change in vehicle acceleration over time is calculated.

According to the above steps, the curve of speed and acceleration over time under 20%–100% constant accelerator pedal opening is analyzed, example Fig. 17. The graph that acceleration of a vehicle varies with engine speed when the pedal is pressed to different degrees is represented in Fig. 18.

By analyzing these curves, the regularity how engine output power responds to changes in driver input is gained. Moreover, the patterns of engine power output at varying engine speeds are illustrated in Fig. 19; the cloud diagram of engine power distribution reveals the relationship of the engine speed and accelerator pedal opening is depicted in Fig. 20; and the variation curve of engine output power in relation to pedal opening at different degrees is depicted in Fig. 21.

From analysis results, the following conclusions are drawn regarding acceleration performance and power output of the engine, which is one of its crucial influencing factors.

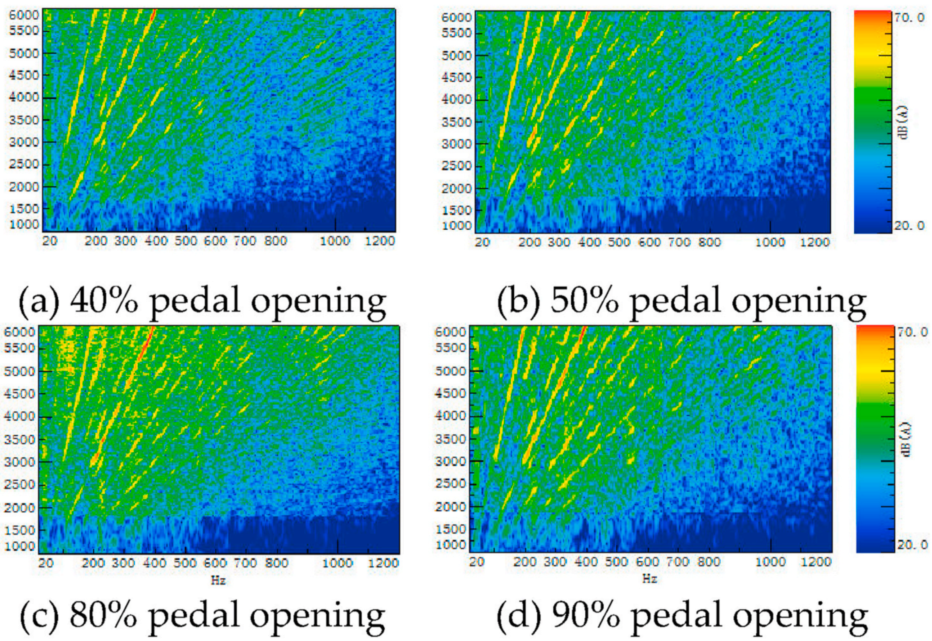


**Fig. 13.** FFT spectrum of sound variation with engine speed.

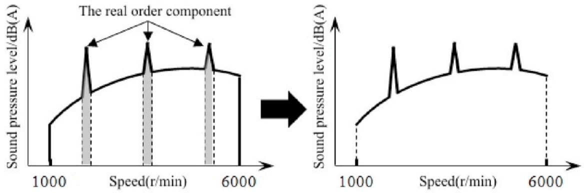


**Fig. 14.** Direct extraction method.

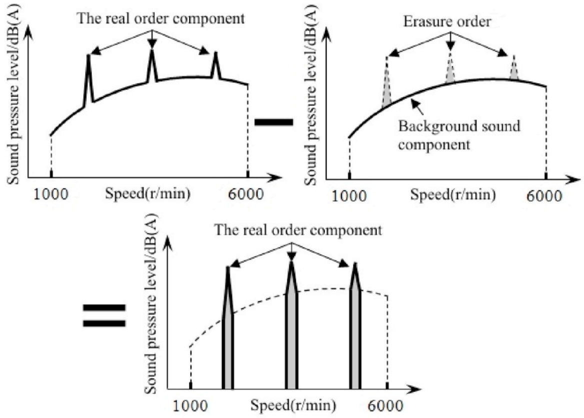


**Fig. 15.** Indirect calculation method.

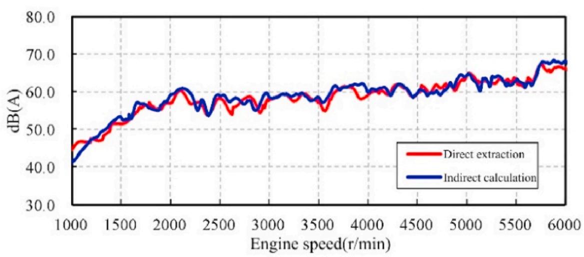


**Fig. 16.** Comparison of engine order amplitudes of the two methods at 40% accelerator pedal opening.

(1) The output power of the engine shows a dramatic rise from the beginning, gradually tends to be flat and decreases slightly, as engine continues to increase in speed at an increasingly rapid rate, which is consistent with characteristics of a typical gasoline engine.
(2) The change in characteristics of vehicle power sensing is reflected during vehicle acceleration while that of engine power sensing by engine output power. The latter is more suitable for vehicle engine order sound correlation analysis.
(3) The acceleration does not demonstrate a totally direct proportion to the force acting on it, which is an important power characteristic of FVs. The different effect on engine order sound caused by this nonlinear variation is a crucial area of study and deserves researchers' close attention.

*3.2.4. Correlation analysis of engine order sound amplitude and power sense*

It is a very complex and systematic process from the accelerator pedal being depressed to the final engine order sound being heard in the vehicle. The amplitude of engine order sound across various operating conditions is summarized by examining the changes in engine speed, as depicted in Fig. 22.

With reference to Fig. 22, the range of engine speeds between 3000 and 6000r/min is an area where engine power experiencing the stable growth; the range of speeds between 1800 and 3000r/min is an area engine power without experiencing major instabilities or disruptions and the range of speeds between 1000 and 1800r/min is an area where engine power undergoes a rapid change as the speed increases within this range.

The sound amplitude produced by the engine at speeds ranging from 3000 to 6000r/min, resulting from an increase in accelerator pedal depression from 20% to 100% is extracted from Fig. 22, and the correlation analysis is conducted with the accelerator pedal

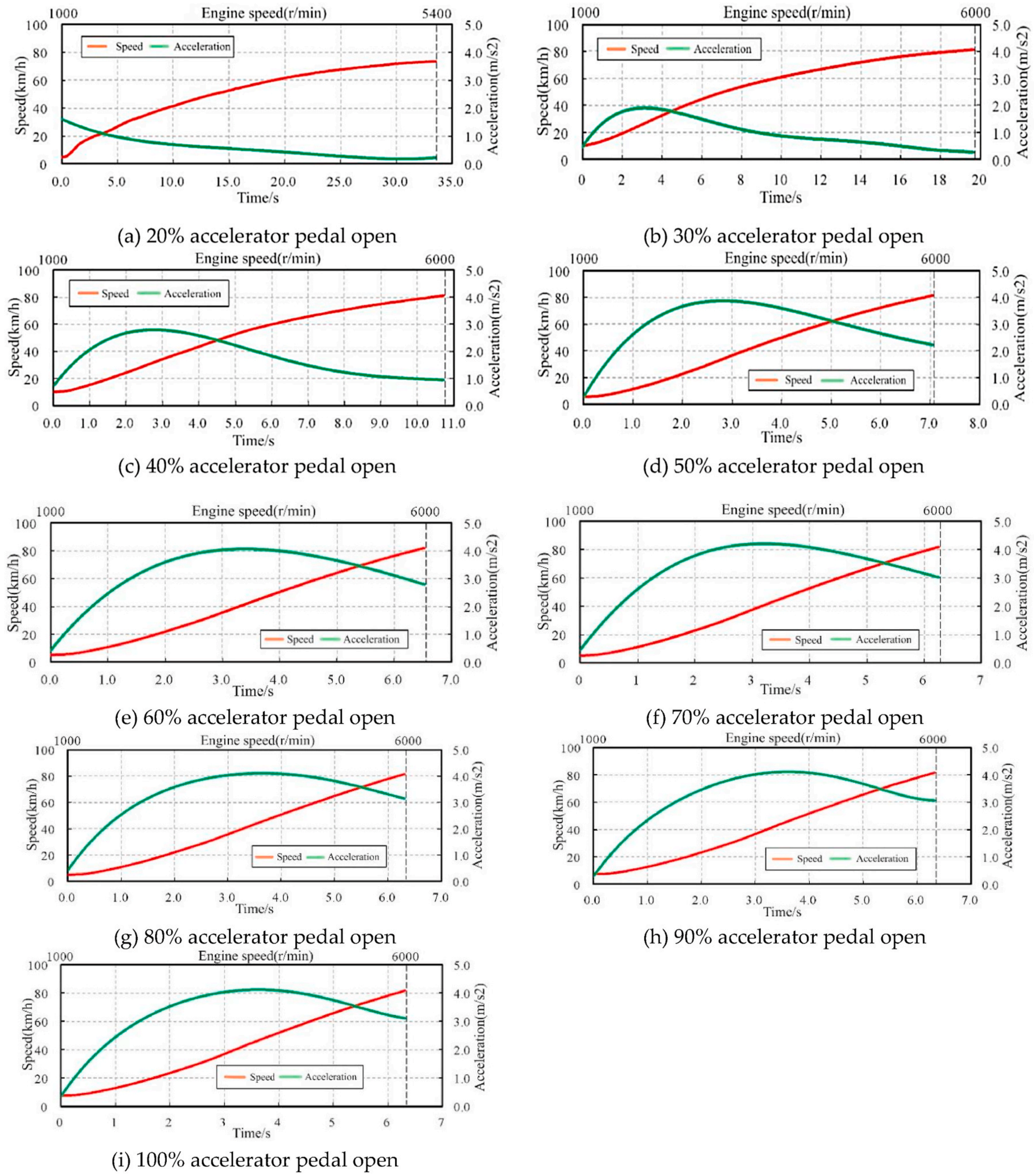


**Fig. 17.** Variation curves of speed and acceleration with time.

opening and engine output power. The mean value of sound amplitude gain coefficient $\alpha_{AVE} = 8.5[dB(A)/100\%]$ is calculated, as listed in Table 3.

### 3.3. Active sound parameter setting

#### 3.3.1. Internal sound and vehicle dynamic characteristics parameters test

Vehicle sound and speed, motor speed, and other parameters are tested to control each accelerator pedal depression. Test conditions are that as vehicle's transmission being put into D gear, the accelerator pedal is quickly pressed and its opening is remained unchanged at 20%; the motor accelerates from 0r/min to 6000r/min; and synchronically information is collected. The range of accelerator pedal opening in above test procedure is within 30%–100%.

The curve in Fig. 23 plots the in-vehicle test results under the conditions that accelerator pedal opening is maintained at 60% and

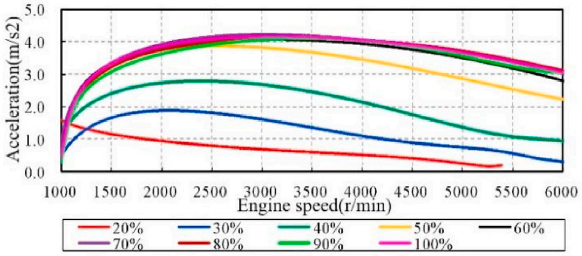


**Fig. 18.** Variation curve of acceleration with engine speed.

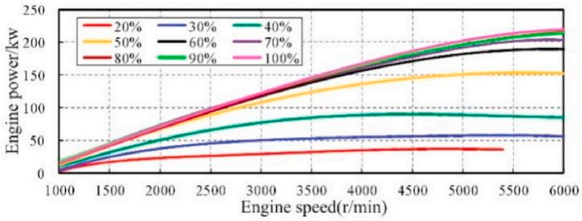


**Fig. 19.** Curve of engine output power with engine speed.

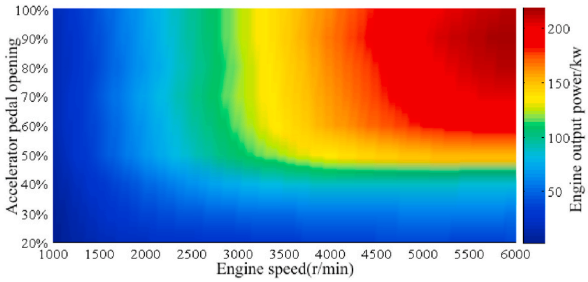


**Fig. 20.** Cloud diagram of engine output power.

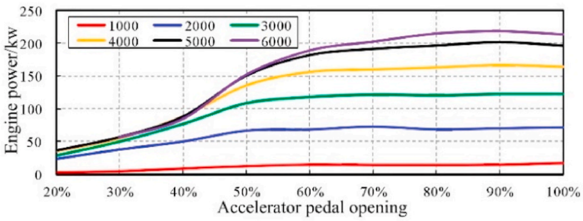


**Fig. 21.** Curve of engine output power at different engine speeds.

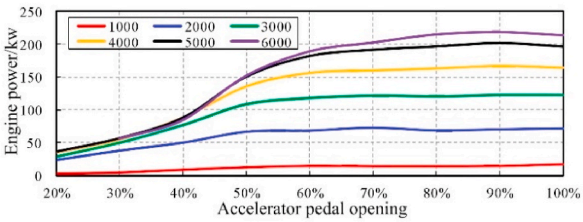


**Fig. 22.** Summary of variation trend of sound amplitude in each condition.

the motor accelerates from 0r/min to 6000r/min.

### *3.3.2. Motor output power analysis*

Referring to the test results of the motor speed and torque, the output power is calculated under the pedal opening of 20%–100%. The graph representation that the power changes with the speed is in Fig. 24, the distribution of power in Fig. 25, and the power varying with accelerator pedal opening in Fig. 26.

Based on the information presented in Fig. 24, initially, the motor output power and motor speed exhibit a linear relationship, with the former increasing in proportion to the latter, and gradually the power tends to remain stable after reaching a certain speed, which shows the consistency with the features of relationships between the power and its speed of rotation.

As illustrated in Fig. 26, a positive correlation between the motor output power and pedal opening is displayed, with the latter increasing stably as the former increases dramatically as the motor speed higher than 3000r/min; there is a direct increase in the power, as the speed is in the range of 1500-3000r/min and accelerator pedal is pressed down to a degree of less than 80% of its maximum possible range of motion; When the motor speed is lower than 1500r/min, the motor output power is linear with the pedal opening in the range higher than 60%.

### *3.3.3. Relationship between sound amplitude and vehicle speed of ASGS in vehicle*

According to Fig. 26 and the actual control situation, the approach used to adjust the sound amplitude depending on the degree the accelerator pedal is pressed,example Fig. 27.

The vehicle speed of 24 km/h corresponds to virtual engine speed of 1800r/min, which is regarded as the inflection point of speed. For FVs in Fig. 27, a minimum low level of vibration is evident in the absence of engine function; the engine order sound amplitude first rise sharply when the engine speed is less than 1800r/min, and then remains at a certain level When the engine speed is greater than 1800r/min, as Fig. 28 illustrated that sound amplitude is controlled based on the vehicle speed. In addition, the minimal degree of vibratory activity requires has necessity to be adjusted conditioned by subjective listening effect in an actual vehicle.

Before the inflection point, the sound amplitude should to "faded in", and the sound is mainly comfortable at this time. After the inflection point, the sound shows a combination of comfort and power.

Through the control of vehicle speed by monitoring the position of accelerator pedal, the ASGS is capable of controlling amplitude of different sound and providing corresponding feedback.

## 4. Research on calibration method of EVs ASGS

### *4.1. Frequency response test of EVs onboard sound system*

The characteristics of frequency response of a sound system can exert a significant influence on the perception of sounds by a driver and on the overall auditory experience of a vehicle, it is thus necessary to test the frequency response of the audio system.

The EV used in the study is parked stationary in the semi-anechoic room, and the controller arrangement is depicted in Fig. 29.

The white noise signal with a time length of 6s is played through the vehicle audio speaker. The original white noise time domain semaphore is depicted in Fig. 30.

Considering the impact of the real vehicle scene, the reflection of the sound wave of the driver and the sound absorption of clothes on the test results, an experimenter is arranged to sit at the driver's position to gather more real frequency response data. In the test, all doors and windows remained close at all times. The noise signal acquired from the measuring point of the vehicle microphone is depicted in Fig. 31. The tested sound signal and the original white noise signal are analyzed by FFT spectrum, as shown in Figs. 32–33.

A conclusion can be drawn from the comparison in Figs. 32–33:

The amplitude of white noise is stable within the range of 20–2000Hz. In the frequency response from the speaker of the audio

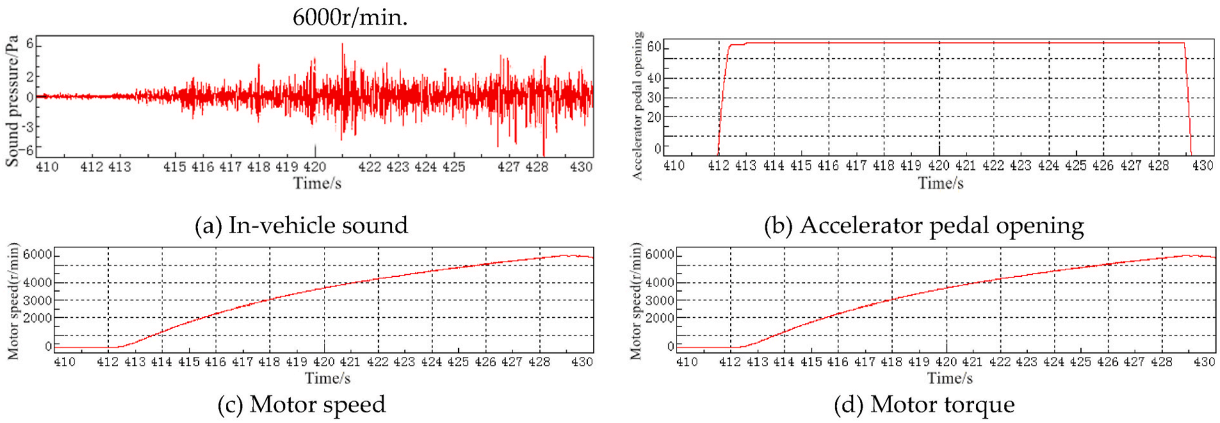


**Fig. 23.** Test signal time curve at 60% accelerator pedal opening.

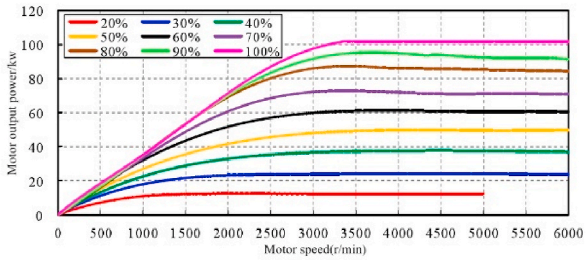


**Fig. 24.** Motor output power curve.

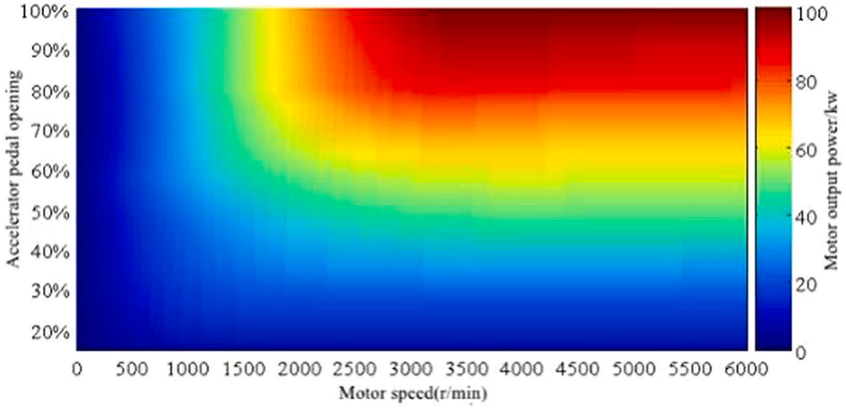


**Fig. 25.** Motor output power cloud diagram.

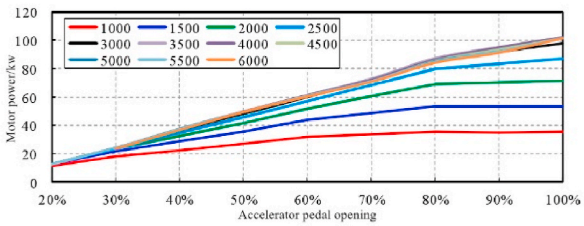


**Fig. 26.** Motor output power Curve at different motor speeds.

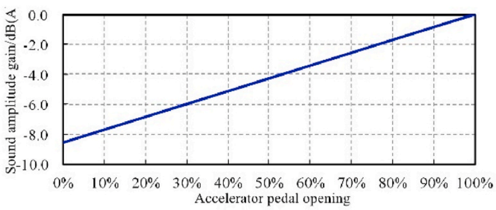


**Fig. 27.** Sound amplitude gain curve.

system to the right ear of the driver, there is a rather obvious sound transmission loss in the vicinity of 300Hz and the range of 480–600Hz, and the sound amplitude within the frequency range of below 100Hz is notably higher when compared to other frequency bands.

## *4.2. High fidelity speaker frequency response test*

The measurement being conducted takes place in the semi-anechoic chamber to eliminate unwanted echoes and reflections. The

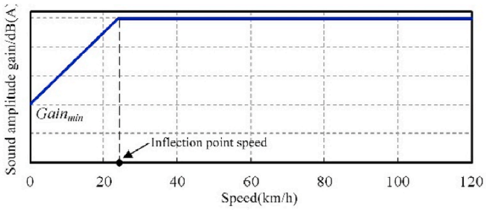


**Fig. 28.** Curve of sound amplitude gain.

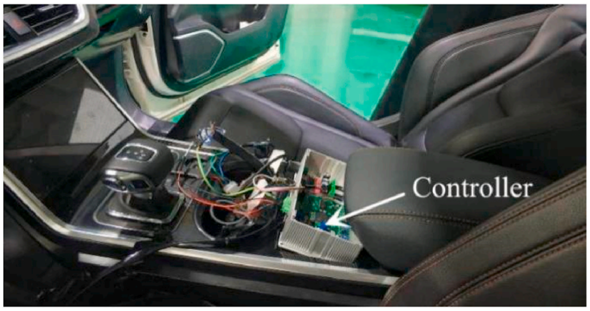


**Fig. 29.** Frequency response test controller of vehicle audio speaker.

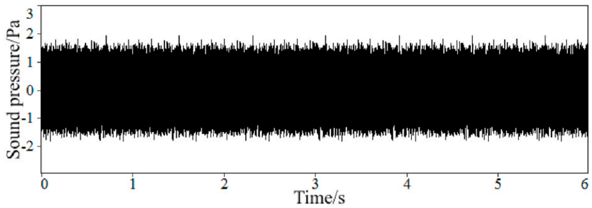


**Fig. 30.** Original white noise time domain signal.

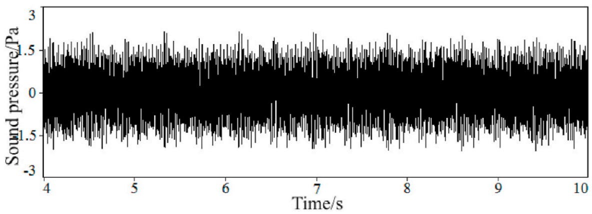


**Fig. 31.** In-vehicle test noise signal.

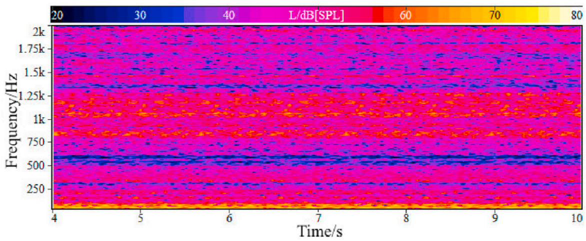


**Fig. 32.** In-vehicle test sound signal FFT spectrum.

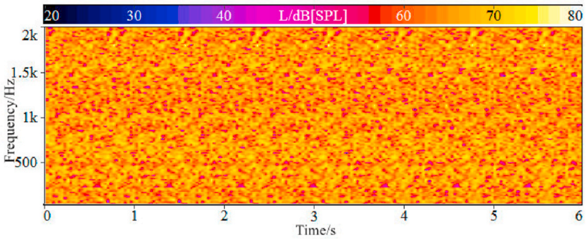


**Fig. 33.** Original white noise FFT spectrum.

model 8030B dual power amplifier active speaker is used as the high-fidelity speaker. A B&K1890A ICP microphone is positioned at a distance of 0.1 m from the surface of speaker to measure the response of speaker, as shown in Fig. 34.

The waveform that represents the audio signal in terms of amplitude and time is employed to assess the performance of high-fidelity speaker, depicted in Fig. 35, the FFT for the waveform is demonstrated in Fig. 36.

Concluded from resulting measurements plotted on the graphs above, high fidelity speaker is capable of reproducing the low and middle frequency components within 20–2000Hz of the white noise signal, yet the amplitude from high fidelity sound reproduction to a certain extent differs from that of original sound, due to the amount the volume or intensity of the sound is adjusted and the location the sound is measured and recorded. Manifestly, the speaker has a high level of accuracy in reproducing the sound frequency characteristics of engine order sound generated by ASGS ranging from 20 to 2000Hz.

## 5. Research on control method of EVs ASGS

### 5.1. Sound fitting

Compared with FVs, the sound of EVs under accelerating conditions lacks the engine order components mainly characterized by medium and low frequencies, and yet possesses the motor order components with high frequencies and the gear engagement order components. Fig. 37 compares the sound spectrum during acceleration.

To gain inside into the sound signals of the engine that varies over time in the vehicle requires assistance from the STFT method, which is a method extended from discrete Fourier transform. Window function information, as can be seen in Table 4.

Kaiser window function is a versatile tool in processing and analyzing digital signal, for it is able to adjust the width of main lobe to capture the amount signal is captured by the function and to adjust the peak value of side lobe to filter out unwanted signals by controlling the shape parameter $\beta$ and window length $N$.

Fig. 38 shows that the sound signal captured inside the FV tested on a flat asphalt pavement, is processed by FFT algorithm.

Depending on the STFT, the engine order components and window Kaiser function are analyzed within main parameters that are set as follows: $\beta$ is 5.8, window length 1280, FFT length 4096, overlap rate 50%, and time frame length 0.05s. Fig. 39 represents that the sound signal collected inside the vehicle that accelerates is analyzed in terms of its frequency components.

According to sound spectra under acceleration in Figs. 38–39, the variation pattern of amplitude in the main energy region and order components shares marked similarity with that in original input signals, whereas the subtle difference exists in the low-speed and high-order sub-region, and the discontinuity, to some extent, in some order components.

Subjective audition confirms that the dissimilarities between subjective hearing of synthesized and original sound are negligible, although the fact that the synthesized is slightly different from the original sound signal, which is attributable to the synthesis error of the engine order component in the high frequency region. Apparently, the STFT and synthesis technique depending on the Kaiser window function is able to accurately simulate the order sound and ASGS sound.

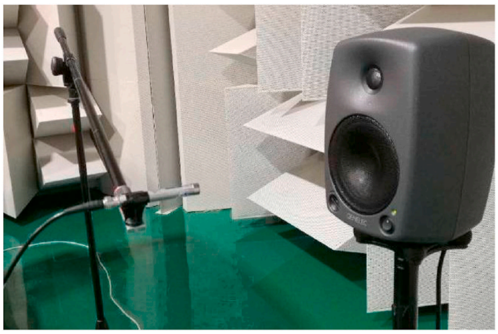

**Fig. 34.** High fidelity speaker frequency response test.

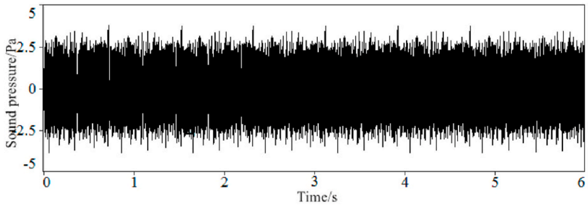


**Fig. 35.** High fidelity speaker test time domain signal.

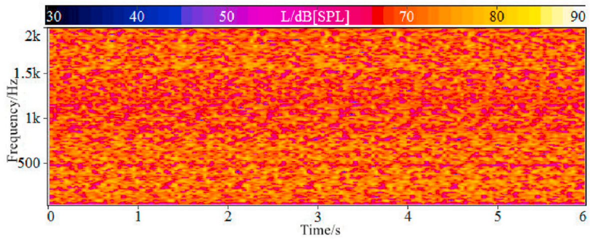


**Fig. 36.** High fidelity speaker test FFT spectrum.

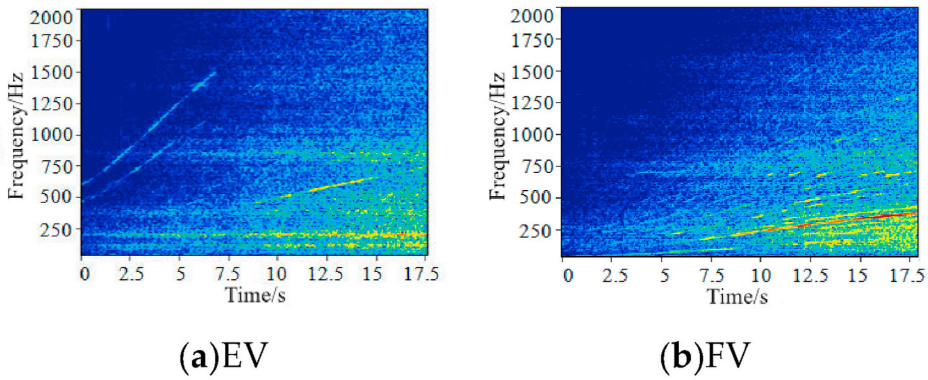


**Fig. 37.** Acoustic spectra in the vehicle under different accelerated driving conditions.

**Table 4**
Window function information.

| Window function | Main lobe width(rad) | Sidelobe peak(dB) | Stopband minimum attenuation(dB) |
|---|---|---|---|
| Rectangular window | 4π/N | −13 | 21 |
| Hanning window | 8π/N | −31 | 44 |
| Hamming window | 8π/N | −41 | 53 |
| Blackman window | 12π/N | −57 | 74 |
| Kaiser window | Can be adjusted | Can be adjusted | Can be adjusted |

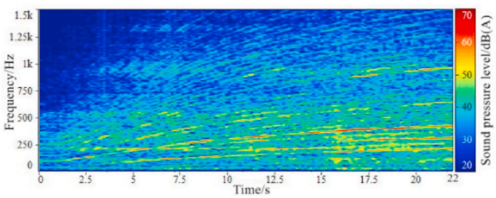


**Fig. 38.** Sound spectrum of an FV accelerating.

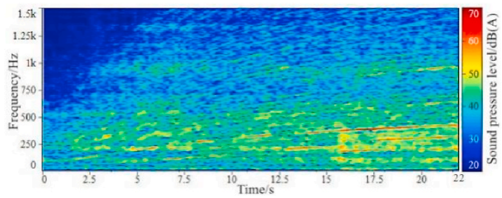


**Fig. 39.** Synthesizes the sound spectrum under accelerated driving.

## 5.2. *Development of ASGS*

### 5.2.1. *Principle and hardware of ASGS*

The ASGS takes readings from the CAN, encompassing the speed of the vehicle, engine speed, the gear, pedal opening and other information in real time. With the aid of the designed sound parameter file, it calculates and synthesizes the corresponding sound signal in the current working context in real time, and transmits the signal to an audio system by way of a power amplifier. The theory framework of ASGS and the actual circuit board are demonstrated in Figs. 40 and 41.

### 5.2.2. *Hardware audio signal testing*

In order to ensure that the ASGS can work stably, the audio signals are tested, as shown in Fig. 42.

According to the test results, the peak value of the square wave of the audio signal is about 5V, which meets the design requirements.

### 5.2.3. *Software design*

C program is utilized to engineer the vehicle's ASGS software. For the purpose of an organized structure and effective debugging, the program is divided into separate modules The software workflow of ASGS in EVs,example Fig. 43.

## 5.3. *Construction*

Amplifier: The audio amplifier is placed in the vehicle and connected to the six speakers using a set of wires.

Speakers: Two low-frequency speakers are placed in the front door, as shown in Fig. 44. Two full-frequency speakers are placed in the rear door, as depicted in Fig. 46. Two high-frequency speakers are placed at the handover position between pillar A, as demonstrated in Fig. 48. The graphs of frequency response of speakers are represented in Figs. 45, 47 and 49, respectively.

From the analysis of the frequency response curve of the speakers, it is discernible that 6 speakers of the EV sound system can reproduce the engine order sound of the ASGS with high fidelity over in the frequency interval of 20–2000Hz.

## 5.4. *ASGS sound synthesis accuracy verification*

The input signal of the virtual engine speed is configured to have the same characteristics as that in Scheme 3. To be specific, the engine speeds up from 1000r/min to 6000r/min, the pedal opening is 100%, and the high-fidelity speaker volume knob is regulated to the position corresponding to the sound amplitude specified in Scheme 3; furthermore, the sound signal is tested through the manipulation of virtual engine speed. The time-domain signal obtained from the high-fidelity speaker playback test to simulate audio landscape during acceleration within the vehicle is revealed in Fig. 50, and the time-domain signal of the original design state of the

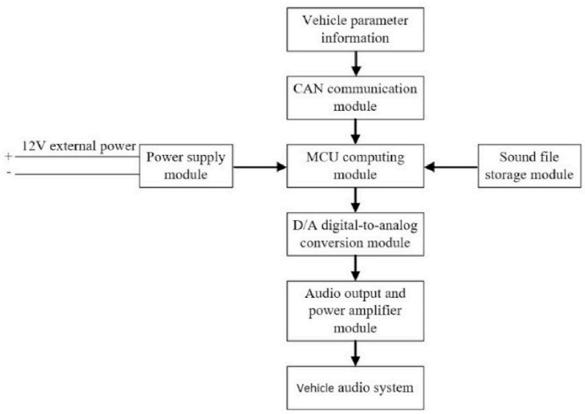


**Fig. 40.** Schematic diagram of in-vehicle ASGS.

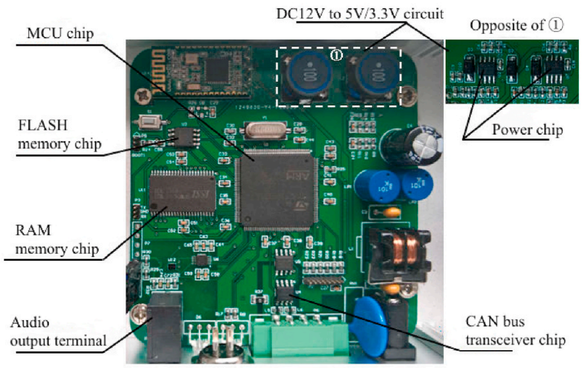


**Fig. 41.** Real picture of the main circuit board of the active sound controller.

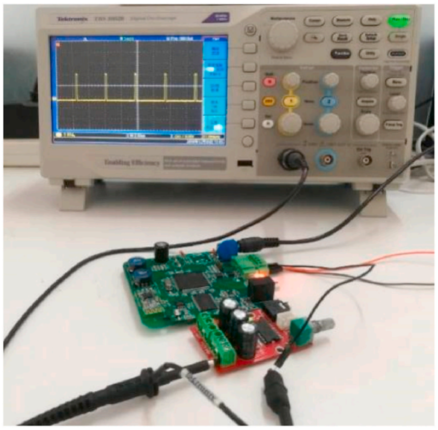

**Fig. 42.** Audio signal test.

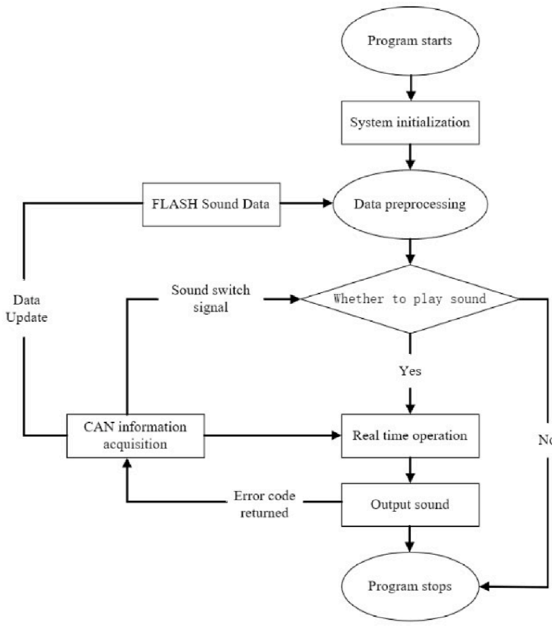


**Fig. 43.** ASGS working flow chart.

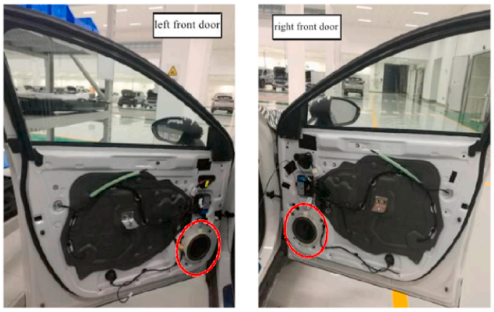


**Fig. 44.** Low frequency speaker.

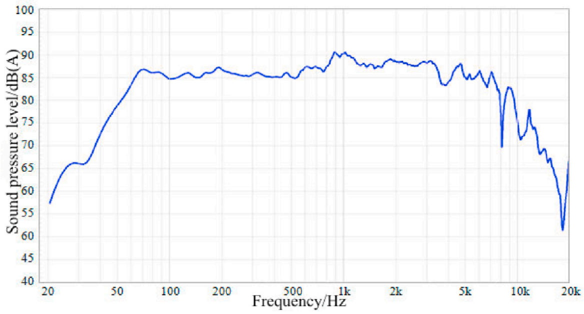


**Fig. 45.** Frequency response curve of low-frequency speaker.

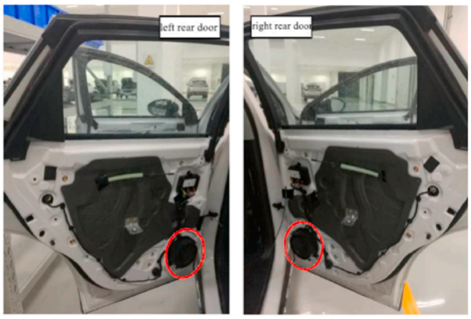


**Fig. 46.** Full frequency speaker.

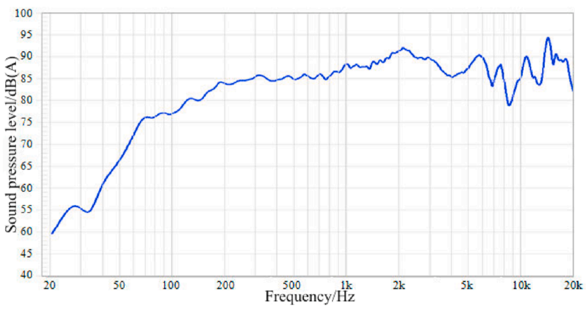


**Fig. 47.** Frequency response curve of full-frequency speaker.

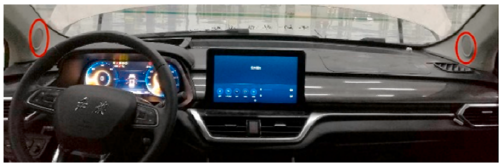

**Fig. 48.** High-frequency loudspeaker.

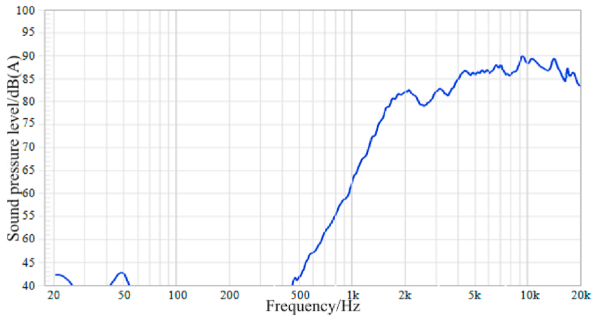


**Fig. 49.** Frequency response curve of high frequency speaker.

acoustic environment during vehicular acceleration in Scheme 3 is presented in Fig. 51. Subsequently, the comparison between spectra of the reconstructed and the original is illustrated in Fig. 52.

Observably, the two time-domain signals are basically consistent with each other, but slightly different in 15–18s. In the test of subjective evaluation, the engine sound is stable regardless of the changes in two different conditions. From the spectral analysis, the sound synthesized by the ASGS, therefore, is capable of precisely regenerate sound spectrum characteristics of the design state.

### 5.5. Sound calibration and target achievement verification of real vehicle static active vocal system

#### 5.5.1. Simulated acceleration condition

The sound amplitude of a vehicle with different accelerator positions is changing, influenced by the increase of speed, as presented in Fig. 53. The variation of the sound amplitude target under specific conditions of full throttle is depicted in Fig. 54. The graph of actual sound amplitude gain of the original sound system at each virtual engine speed is represented in Fig. 55. FFT spectra for analyzing sound reproduced by high-fidelity speaker and original sound system under 100% pedal opening, are shown in Fig. 56.

According to Figs. 53–56, overall, the change curve of the original vehicle audio sound amplitude and hi-fi loudspeaker verification results displays a significant level of consistency with the target line. The general direction of sound amplitude at each engine speed exhibits a linear increase, in response to alterations in accelerator pedal opening.

The frequency response from the whole sound system to the driver's ear needs the mutual cooperation between the speakers, and the sound system power amplifier and algorithm are used for comprehensive control.

#### 5.5.2. Simulated acceleration condition

Under the static condition of real vehicle, the test result acquired when the sound system of the original vehicle simulates uniform speed working condition is shown in Fig. 57.

In low and medium engine speed areas, the sound amplitude from original system is more obvious, whereas in the high-speed zone, the amplitude of the system is moderate, which can ensure low intensity of a sound when driving at a constant speed.

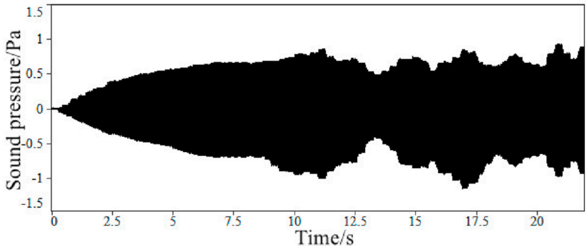


**Fig. 50.** Time domain signal of simulating accelerated driving.

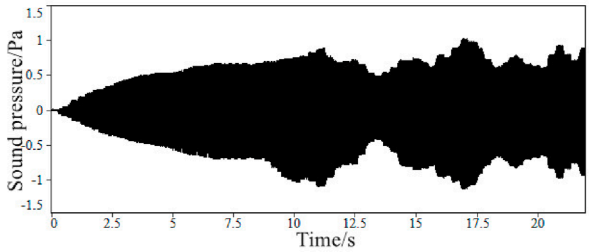


**Fig. 51.** Time domain signal under Scheme 3.

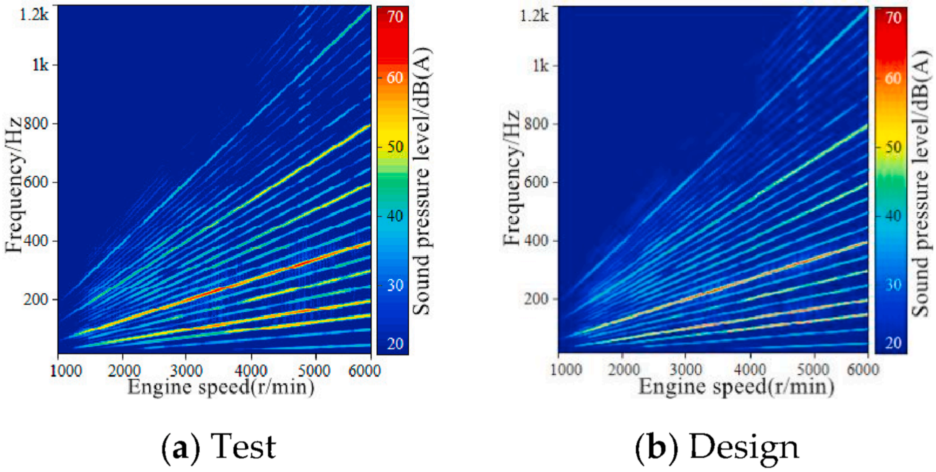


**Fig. 52.** FFT spectra of two state sounds.

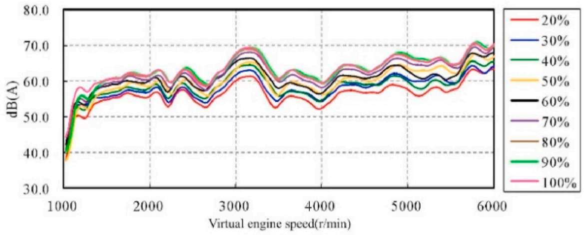


**Fig. 53.** Curve of sound amplitude gain.

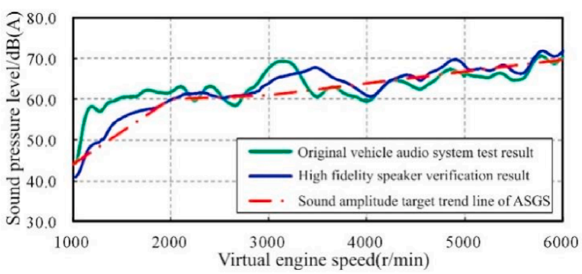


**Fig. 54.** Sound amplitude change curve of the original system under simulated acceleration conditions.

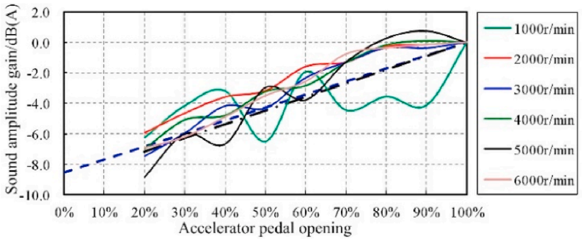


**Fig. 55.** Actual sound amplitude gain curve of the original system.

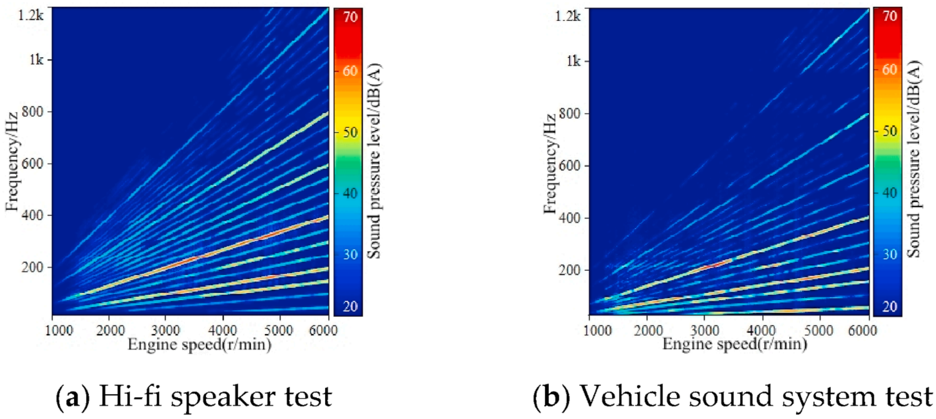


**Fig. 56.** Comparison of simulated accelerated driving engine sounds at 100% pedal opening.

## 6. Test and discussion

### 6.1. Objective test

#### 6.1.1. Accelerated driving condition

In the state when ASGS is working and not working, the sound signal at the position of the driver's right ear is tested during the acceleration process at 100% pedal opening. The general shape that SPL of the three kinds of sound volume, the first two produced by an EV with the ASGS operational and inoperative, the third being the desired volume, varies as virtual engine speed rises and the comparison of FFT spectrum under the two states of ASGS are shown in Figs. 58–60.

According to Figs. 58–60, the change curve of total value with ASGS operating normally can generally follow the target trend line. The ASGS basically fulfills the sound design requirements for both comfort quality and power sense quality.

#### 6.1.2. Constant speed condition

The sound signal of the ASGS is tested at a uniform velocity, under the virtual speed of 1000r/min-6000r/min, from which sound pressure levels of the different states are calculated and compared as shown in Figs. 61 and 62.

With reference to the graphs, the change trend of the SPL in the vehicle with its ASGS operational is basically the same as that of target value, which guarantees the noise level in low intensity, so as to meet the comfort quality goal requirements of uniform driving. The sharpness tested when the system is in operation is less than when the system is not in operation, for at a speed of 28.6 km/h, the former is no more than 1acum, unlike the latter.

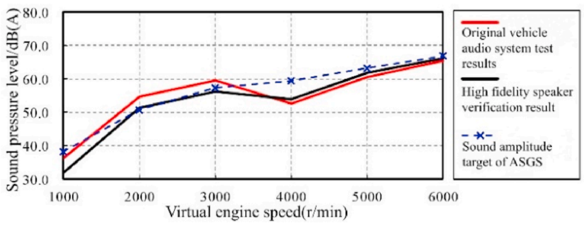


**Fig. 57.** Sound amplitude reaching standard under uniform speed.

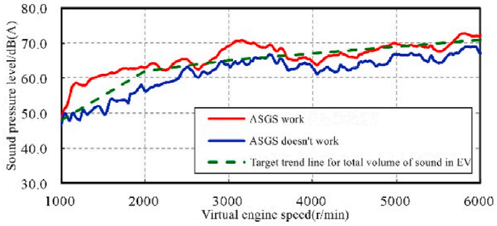


**Fig. 58.** Total sound value curve of 100% pedal opening acceleration driving.

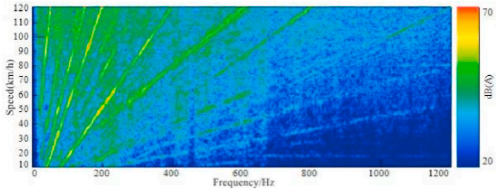

**Fig. 59.** FFT spectrum of ASGS in normal operation.

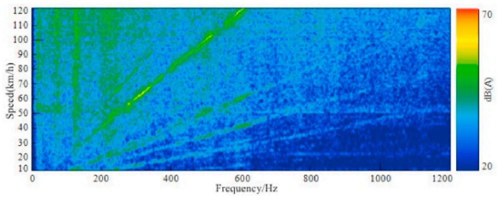

**Fig. 60.** FFT spectrum when ASGS is stopped.

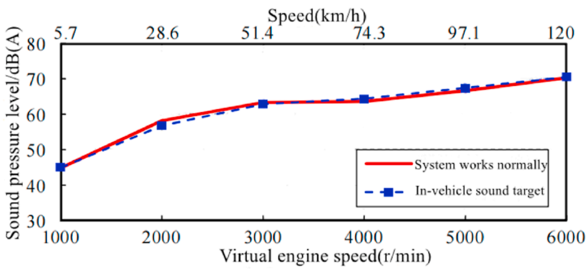


**Fig. 61.** Sound pressure level at uniform speed.

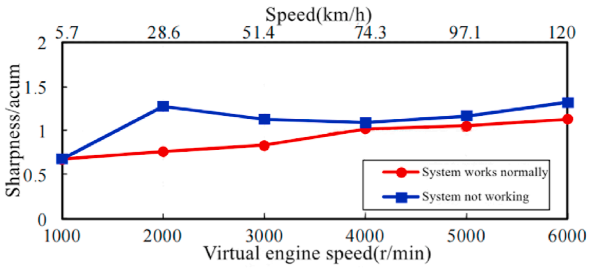


**Fig. 62.** Sound sharpness at uniform speed.

### *6.2. Actual vehicle evaluation*

The sounds inside the EVs and a coupe-type FV, all vehicles in active operation, are analyzed depending on subjective evaluation. The evaluation results of the vehicles are depicted in Figs. 63–64.

Combined with test results assessed subjectively and objectively, it is manifested that the engine order sound the ASGS generates can reduce the magnitude of order components in the high-frequency range and improve the overall comfort level of the sound during acceleration while driving. In the local range, the engine order composition is advanced to achieve the power sense of sound. Furthermore, the level of perceived comfort and power is augmented when a constant velocity is maintained, when the sound amplitude is moderate, and the acoustic sharpness of the sound is increased.

Therefore, the ASGS system of the EV enables the overarching vision for sound control design that balances and optimizes sound quality of comfort and power to be accomplished.

## 7. Conclusion

(1) The concept design goal of providing “a harmonious sound quality with both comfort and dynamic" was formulated, whose technical route was also determined. For the actualization of the goal, a reliable guideline for sound design was developed, in which three dimensions including engine order composition, energy distribution, and sound amplitude enhancement were comprehensively taken into consideration. In addition, for a purpose of providing an objective standard of the sound design scheme’s effectiveness, the total sound value target was set.
(2) Specifically, for discovering how the engine sound is in connection with the vehicle’s dynamic characteristics, the sound parameters were studied; and for discerning how engine order sound amplitude is in association with the power sense, the sound extraction method was analyzed.
(3) In an effort to study the calibration method for the system of ASGS in EVs, the frequency response of on-board sound system and high-fidelity speaker was tested to examine that the engine order sound generated by the ASGS can be utilized to confirm the fitting accuracy and calibrate the sound amplitude simulation.
(4) With the aim of completing the sound fitting, the ASGS in EVs was designed, in which the EV ASGS based on the acoustic output device of audio system was constructed, the accuracy of the system was verified; in addition, the calibration and target achievement verification under the static condition of the real vehicle were carried out.
(5) On balance, the EV ASGS is capable of accomplishing the goal, which is verified by the combination of the objective and subjective symmetry evaluation on the real vehicle. The results exhibit that the sharpness is reduced and the overall comfort level and power level of the sound are improved when the EV is under acceleration and uniform speed symmetry conditions, and when its ASGS is in operation.

## Data availability

Data included in article/supp. Material/referenced in article.

## CRediT authorship contribution statement

**Shuai Zhang:** Conceptualization, Formal analysis, Validation, Visualization, Writing – original draft, Writing – review & editing. **Yipeng Li:** Conceptualization, Formal analysis, Validation, Visualization, Writing – original draft, Writing – review & editing. **Hang Jiang:** Conceptualization, Writing – original draft, Writing – review & editing. **Feng Xiong:** Data curation, Methodology, Writing – original draft. **Liyou Xu:** Conceptualization, Investigation, Validation, Visualization, Writing – original draft, Writing – review & editing. **Yuntao Cao:** Data curation, Methodology, Writing – original draft.

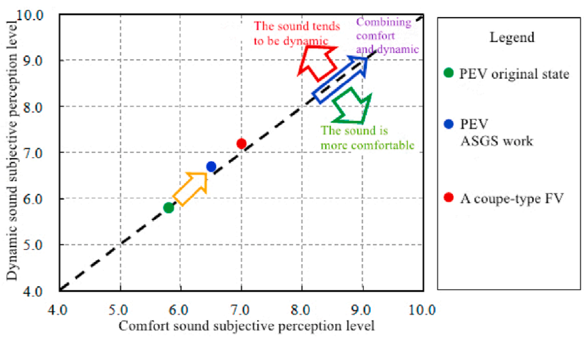


**Fig. 63.** Accelerated conditional quality distribution.

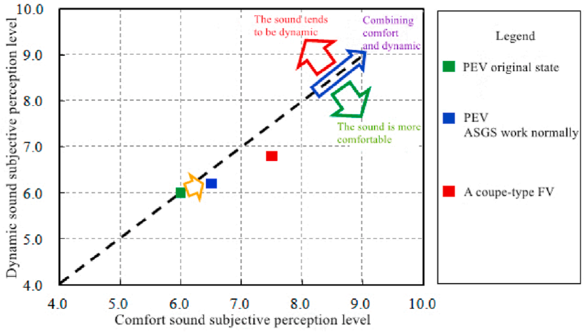


**Fig. 64.** Uniform conditions quality distribution.

## Declaration of competing interest

The authors declare that they have no known competing financial interests or personal relationships that could have appeared to influence the work reported in this paper.


## Acknowledgements

This work was supported by the Key R&D and Promotion Project of Henan Province (no. 232102240052), Science and Technology Research Project of Henan Province (No. 212102310040), Major Science and Technology Project of Henan Province (221100240400), Key Scientific Research Project of Colleges and Universities in Henan Province (No. 21A580003), Special Project for Scientific and Technological Talents of Chongqing Banan District (2020TJZ021), and Natural Science Foundation Project of Chongqing Science and Technology Commission (Grant No. cstc2020jcyjmsxmX0458), National Key Research and Development Program of China (no. 2022YFD2001203).


## References


[1] R. Jiang, Z. Jin, S. Ci, et al., Reliability-based multilevel optimization of carbon fiber-reinforced plastic control arm, Struct. Multidiscip. Optim. 65 (2022) 314, https://doi.org/10.1007/s00158-022-03429-0.

[2] T. Sun, R. Jiang, H. Sun, D. Liu, Z. Pan, Multiscale uncertainty propagation analysis and reliability optimization of the CFRP crossbeam of the twist beam axle, Int. J. Mech. Sci. 242 (2023) 108022, https://doi.org/10.1016/j.ijmecsci.2022.108022.

[3] C. Ma, Y. An, L. Liu, M. Degano, X. Ning, J. Zhang, et al., Sound-quality diagnosis method of permanent magnet synchronous motor for electric vehicles based on critical band analysis, IET Electr. Power Appl. 13 (2019) 1613–1621, https://doi.org/10.1049/iet-epa.2019.0088.

[4] J. Mosquera-Sanchez, M. Sarrazin, K. Janssens, L. deOliveira, W. Desmet, Multiple target sound quality balance for hybrid electric powertrain noise, Mech. Syst. Signal Process. 99 (2018) 478–503, https://doi.org/10.1016/j.ymssp.2017.06.034.

[5] F. Doleschal, J. Verhey, Pleasantness and magnitude of tonal content of electric vehicle interior sounds containing subharmonics, Appl. Acoust. 185 (2021) 108442, https://doi.org/10.1016/j.apacoust.2021.108442.

[6] D. Swart, A. Bekker, The relationship between consumer satisfaction and psychoacoustics of electric vehicle signature sound, Appl. Acoust. 145 (2019) 167–175, https://doi.org/10.1016/j.apacoust.2018.09.019.

[7] V. Wagner-Hartl, B. Graf, M. Resch, P. Langjahr, Subjective evaluation of EV sounds: a human-Centered approach, Adv. Intell. Syst. Comput. 876 (2019) 10–15, https://doi.org/10.1007/978-3-030-02053-8_2.

[8] D. Min, B. Park, J. Park, Artificial engine sound synthesis method for Modification of the acoustic characteristics of electric vehicles, Shock Vib. 2018 (2018) (2018) 5209207, https://doi.org/10.1155/2018/5209207.

[9] Hee, L. Kwon, K. Kim, Objective evaluation of whine noise of electric vehicle according to the characteristics of sound-absorbing materials, Transactions of the Korean Society for Noise and Vibration Engineering 27 (2017) 829–835, https://doi.org/10.5050/KSNVE.2017.27.7.829.

[10] J. Park, H. Park, Y. Kang, A study on sound quality of vehicle engine sportiness using factor analysis, J. Mech. Sci. Technol. 34 (2020) 3533–3543, https://doi.org/10.1007/s12206-020-0805-0.

[11] E. Zhang, L. Hou, C. Shen, Y. Shi, Y. Zhang, Sound quality prediction of vehicle interior noise and mathematical modeling using a back propagation neural network (BPNN) based on particle swarm optimization (PSO), Meas. Sci. Technol. 27 (2016) 015801, https://doi.org/10.1088/0957-0233/27/1/015801.

[12] J. Jeong, I. Yang, A. binAbu, K. Cha, Development of a new sound quality metric for evaluation of the interior noise in a passenger car using the logarithmic Mahalanobis distance, P I Mech Eng D-J Aut 227 (2013) 1363–1376, https://doi.org/10.1177/0954407013495529.

[13] Z. Wang, P. Li, H. Liu, J. Yang, S. Liu, L. Xue, Objective sound quality evaluation for the vehicle interior noise based on responses of the basilar membrane in the human ear, Appl. Acoust. 172 (2020) 107619, https://doi.org/10.1016/j.apacoust.2020.107619.

[14] T. Zhuang, Y.S. Zuo, Research on subjective and objective evaluation of car interior sound quality, Appl. Mech. Mater. 455 (2014) 193–197, https://doi.org/10.4028/www.scientific.net/AMM.455.193.

[15] Y. Lu, Y. Zuo, H. Wang, C. Wu, Sound quality prediction for power coupling mechanism of HEV based on CEEMD-HT and RVM, Neural Comput. Appl. 33 (2021) 8201–8216, https://doi.org/10.1007/s00521-020-04934-3.

[16] Y. Lee, T. Shin, S. Lee, Sound quality analysis of a passenger car based on electroencephalography, J. Mech. Sci. Technol. 27 (2013) 319–325, https://doi.org/10.1007/s12206-012-1248-z.

[17] S. Lee, G. Lee, J. Back, Development of sound-quality indexes in a car cabin owing to the acoustic characteristics of absorption materials, Appl. Acoust. 143 (2018) 125–140, https://doi.org/10.1016/j.apacoust.2018.09.004.

[18] G. Ghanati, S. Azadi, Active control of vehicle's interior sound field by using multichannel H-infinity robust controller, P I Mech Eng D-J Aut 234 (2020) 725–738, https://doi.org/10.1177/0954407019848523.

[19] M. Anthony, C. Chang, S. Kuo, Active Noise Control for Muffler. Asia-Pacific Signal and Information Processing Association Annual Summit and Conference, 2018, pp. 140–144.

[20] W. Chen, C. Lu, Z. Liu, H. Williams, L. Xie, A computationally efficient active sound quality control algorithm using local secondary-path estimation for vehicle interior noise, Mech. Syst. Signal Process. 168 (2022) 108698, https://doi.org/10.1016/j.ymssp.2021.108698.
[21] Y. Wang, L. Gu, F. Liu, M. Dong, Online secondary path modeling for active sound quality control systems, Appl. Acoust. 155 (2019) 44–52, https://doi.org/10.1016/j.apacoust.2019.05.014.
[22] F. Liu, J. Mills, M. Dong, L. Gu, Active broadband sound quality control algorithm with accurate predefined sound pressure level, Appl. Acoust. 119 (2017) 78–87, https://doi.org/10.1016/j.apacoust.2016.12.009.
[23] S. Lee, S. Lee, J. Back, T. Shin, A new method for active cancellation of engine order noise in a passenger car, Appl Sci-Basel 8 (2018) 1394, https://doi.org/10.3390/app8081394.
[24] Y. Wang, H. Guo, Y. Li, N. Liu, C. Yang, Active control for vehicle interior noise based on DWT-FxLMS algorithm using a piezoelectric feedback system, Appl. Acoust. 167 (2020) 107409, https://doi.org/10.1016/j.apacoust.2020.107409.
[25] W. Yu, Analysis and Optimization of Low-Speed Road Noise in Electric Vehicles, Wirel Commun Mob Com, 2021, https://doi.org/10.1155/2021/5537704.
[26] Z. Liu, X. Li, S. Du, W. Chen, J. Shao, Q. Zheng, Strategy and implementing techniques for the sound quality target of car interior noise during acceleration, Appl. Acoust. 182 (2021) 108171, https://doi.org/10.1016/j.apacoust.2021.108171.
[27] T. Feng, G. Sun, J. Xu, M. Li, T. Lim, Frequency domain inverse model LMS algorithm for active sound TUNING system of powertrain noise, in: 22nd International Congress on Sound and Vibration, ICSV), 2015.
[28] S. Wu, External acceleration noise control of electric vehicles based on sound intensity measurement method, International Conference on Measuring Technology and Mechatronics Automation (2021) 414–418, https://doi.org/10.1109/ICMTMA52658.2021.00095.
[29] J. Lee, Y. Park, J. Chan, H. Jang, Development of a sound quality index for the evaluation of booming noise of a passenger car based on regressive correlation, Int J Auto Tech-Kor 6 (2005) 367–374.
[30] F. Zeng, S. Sun, Study on the sound quality of steady and unsteady exhaust noise, Math. Probl Eng. 2018 (2018) 6205140, https://doi.org/10.1155/2018/6205140.
[31] X. Zhang, The Co-pilot position of vehicle noise quality prediction based on SVM, IOP Conf. Ser. Mater. Sci. Eng. 735 (2020) 012064, https://doi.org/10.1088/1757-899X/735/1/012064.
[32] D. Siano, M. Panza, Sound quality analysis of the powertrain booming noise in a Diesel passenger car, Energy Proc. 126 (2018) 971–978, https://doi.org/10.1016/j.egypro.2017.08.189.
[33] S. Moon, S. Park, D. Park, W. Kin, M. Yun, D. Park, A study on affective dimensions to engine acceleration sound quality using acoustic parameters, Appl Sci-Basel 9 (2019) 604, https://doi.org/10.3390/app9030604.